Glucose Transporter Function Is Controlled by Transporter Oligomeric Structure. A Single, Intramolecular Disulfide Promotes GLUT1 Tetramerization†

Ralph J. Zottola, Erin K. Cloherty, Peter E. Coderre, Antony Hansen,‡ Daniel N. Hebert,§ and Anthony Carruthers*

Department of Biochemistry and Molecular Biology, Program in Molecular Medicine, University of Massachusetts Medical School, Two Biotech, 373 Plantation Street, Worcester, Massachusetts 01605

Received March 13, 1995; Revised Manuscript Received April 25, 1995⊗

ABSTRACT: The human erythrocyte glucose transporter is an allosteric complex of four GLUT1 proteins whose structure and substrate binding properties are stabilized by reductant-sensitive, noncovalent subunit interactions [Hebert, D. N., & Carruthers, A. (1992) *J. Biol. Chem. 267,* 23829−23838]. In the present study, we use biochemical and molecular approaches to isolate specific determinants of transporter oligomeric structure and transport function. When unfolded in denaturant, each subunit (GLUT1 protein) of the transporter complex exposes two sulfhydryl groups. Four additional thiol groups are accessible following subunit exposure to reductant. Assays of subunit disulfide bridge content suggest that two inaccessible sulfhydryl groups form an internal disulfide bridge. Differential alkylation/peptide mapping/N-terminal sequence analyses show that a GLUT1 carboxyl-terminal peptide (residues 232−492) contains three inaccessible sulfhydryl groups and that an N-terminal GLUT1 peptide (residues 147−261/299) contains two accessible thiols. The carboxyl-terminal peptide most likely contains the intramolecular disulfide bridge since neither its yield nor its electrophoretic mobility is altered by addition of reductant. Each GLUT1 cysteine was changed to serine by oligonucleotide-directed, *in vitro* mutagenesis. The resulting transport proteins were expressed in CHO cells and screened by immunofluorescence microscopy for their ability to expose tetrameric GLUT1-specific epitopes. Serine substitution at cysteine residues 133, 201, 207, and 429 does not inhibit exposure of tetrameric GLUT1-specific epitopes. Serine substitution at cysteines 347 or 421 prevents exposure of tetrameric GLUT1-specific epitopes. Hydrodynamic analysis of GLUT1/GLUT4 chimeras expressed in and subsequently solubilized from CHO cells indicates that GLUT1 residues 1−199 promote chimera dimerization and permit GLUT1/chimera heterotetramerization. This GLUT1 N-terminal domain is insufficient for chimera tetramerization which additionally requires GLUT1 residues 200−463. Extracellular reductants (dithiothreitol, β-mercaptoethanol, or glutathione) reduce erythrocyte 3-*O*-methylglucose uptake by up to 15-fold. This noncompetitive inhibition of sugar uptake is reversed by the cell-impermeant, oxidized glutathione. Reductant is without effect on sugar exit from erythrocytes. Dithiothreitol doubles the cytochalasin B binding capacity of erythrocyte-resident glucose transporter, abolishes allosteric interactions between substrate binding sites on adjacent subunits, and occludes tetrameric GLUT1-specific GLUT1 epitopes *in situ.* CHO cell-resident GLUT1 structure and transport function are similarly affected by extracellular reductant. We conclude that each subunit of the glucose transporter contains an extracellular disulfide bridge (Cys347 and Cys421) that stabilizes transporter oligomeric structure and thereby accelerates transport function.

Protein-mediated solute transport across cell membranes is a fundamental but incompletely characterized biological process mediated by two broad classes of transport mechanism (Stein, 1986). The channel mechanisms function as membrane-spanning pores (Stein, 1986). The carrier mechanisms (uniporters, symporters, and antiporters) are comprised of one or more members of a family of "E1·E2" catalytic subunits that cycle between two conformational states. The "E1" state exposes a solute export site, and the "E2" state exposes a solute import site. No single subunit can exist in both E1 and E2 states simultaneously (Stein, 1986). Cells exploit this conformational cycle to effect carrier-mediated solute transport. Solute binds to the E1 or E2 conformer and is translocated during the E1 ↔ E2 conformational change. With some carriers (e.g., uniporters), cycling is constitutive and solute binding is without effect on the rate of E1 ↔ E2 isomerization. In other instances, solute binding accelerates (e.g., uniporters, antiporters, or symporters) or is required to promote the E1 ↔ E2 conformational change (e.g., antiporters and symporters).

Although E1 or E2 carrier conformers have not been visualized directly, some proposed transport cycle intermediates have been isolated. For example, the Na,K-ATPase (a primary active E1·E2 antiporter that requires ATP hydrolysis for productive conformational change) has been isolated with occluded (bound but inaccessible) Na^+ or Rb^+ (Glynn et al., 1984; Glynn & Richards, 1982). Other proposed steps have precedent in enzyme catalysis. Yeast hexokinase, for example, undergoes significant conformational change upon glucose binding that engulfs the bound sugar (Anderson et

† This work was supported by NIH Grants DK 44888 and DK 36081.

* Author to whom correspondence should be addressed. Internet address: tc@unmassmed.ummed.edu. Phone: 508-856-5570. FAX: 508-856-4289.

‡ Current address: Department of Clinical Pharmacology, Flinders Medical Centre, Bedford Park, South Australia 5042, Australia.

§ Current address: Department of Cell Biology, Yale University Medical School, New Haven, CT.

⊗ Abstract published in *Advance ACS Abstracts,* June 15, 1995.

0006-2960/95/0434-9734$09.00/0

al., 1979). Similar conformational changes are suggested to promote substrate occlusion and translocation in the E1•E2 transporters (Barnett et al., 1973; Stein, 1986; Widdas, 1952).

The catalytic subunit of the human erythrocyte sugar transporter (a passive uniporter) is the erythrocyte glucose transport protein (GLUT1) (Baldwin et al., 1979; Kasahara & Hinkle, 1977; Mueckler et al., 1985). In isolation, each GLUT1 protein functions as an E1•E2 carrier (Appleman & Lienhard, 1989; Baldwin et al., 1982). Several independent lines of evidence demonstrate that *in situ*, the glucose transporter is a GLUT1 homotetramer (Hebert & Carruthers, 1991, 1992; Jarvis et al., 1986; Jung et al., 1980; Pessino et al., 1991; Zoccoli et al., 1978) and that the kinetics of transport differ fundamentally from those expected of an E1•E2 carrier. Rather than exposing import and export sites sequentially, the erythrocyte sugar transporter appears to expose import and export sites simultaneously (Baker & Naftalin, 1979; Carruthers, 1986a, 1991; Chin et al., 1992; Hebert & Carruthers, 1991, 1992; Helgerson & Carruthers, 1987; Janoshazi et al., 1991; Janoshazi & Solomon, 1993; Naftalin, 1988; Naftalin & Rist, 1994). One hypothesis that accounts for this behavior suggests that subunits of tetrameric GLUT1 behave as E1•E2 carriers in isolation but present conformational states with a pseudo-*D2* symmetry in the parental structure (Hebert & Carruthers, 1992). If one subunit exists in an E2 state, the adjacent subunit must adopt the E1 state. Thus, the transporter contains two E1 conformers and two E2 conformers at all times. If an E2 subunit binds and translocates substrate, the adjacent E1 subunit must undergo the antiparallel conformational change regardless of occupancy state. In this way, the transporter is transformed from one where import and export sites are mutually exclusive (the E1•E2 paradigm) to one where sugar import and sugar export sites coexist (but only on different subunits) and interact cooperatively.

The molecular interactions that stabilize tetrameric GLUT1 are only partly understood. Exposure to reductant causes tetrameric GLUT1 to dissociate into GLUT1 dimers, but subunits of tetrameric GLUT1 are not attached via disulfide bridges (Hebert & Carruthers, 1992). Each subunit of SDS-denatured tetrameric GLUT1 exposes only two thiols (Hebert & Carruthers, 1992) while reduced denatured GLUT1 exposes all six sulfhydryl groups (Baldwin et al., 1982; Hebert & Carruthers, 1992). This suggests that glucose transporter oligomeric structure and cooperative catalytic function result from noncovalent interactions promoted or stabilized by intramolecular disulfide bridges.

In the current study, we use biochemical and molecular approaches to test this hypothesis. Our results support the hypothesis that a single intramolecular disulfide bridge (cysteine residues 347 and 421) spans the catalytic domain of each subunit. This promotes GLUT1 tetramerization, cooperative interactions between substrate binding sites of adjacent subunits, and transport acceleration.

MATERIALS AND METHODS

Materials. [^{3}H]Cytochalasin B, [^{3}H]-3-*O*-methylglucose, [^{14}C]-2-deoxy-D-glucose, [^{14}C]iodoacetic acid, and [^{125}I]-protein A were purchased from New England Nuclear. Rabbit antisera raised against a synthetic carboxyl-terminal peptide of GLUT1 (intracellular residues 480−492; C-Ab) were obtained from East Acres Biologicals. Anti-GLUT1 antisera reacting exclusively with extracellular epitopes of GLUT1 (δ-Ab) were prepared as described previously (Harrison et al., 1990a). Fluorescein- and rhodamine-conjugated secondary antibodies were purchased from Calbiochem. Recently expired human blood was obtained from the University of Massachusetts Medical Center Blood Bank. Reagents were purchased from Sigma Chemicals. Restriction enzymes were purchased from New England Biolabs. Fetal bovine serum was purchased from UBI. Sculptor was purchased from Amersham Life Science Inc. and DOTAP from Boehringer Mannheim. Media, trypsin, antibiotics, and G418 were purchased from Gibco and CHO-K1 cells and pRSVneo from American Type Tissue Culture. Plasma membranes from Chinese hamster ovary (CHO) cells and from 3T3-L1 adipocytes were generously provided by Drs. A. Pessino, S. A. Harrison, and M. P. Czech.

Solutions. Saline consisted of 150 mM NaCl, 5 mM Tris-HCl, and 0.2 mM EDTA, pH 7.4. Lysis medium contained 10 mM Tris-HCl, 2 mM EDTA, pH 7.4. Stopper solution consisted of saline (4 °C) plus 10 μM cytochalasin B and 10 μM $HgCl_2$. Tris medium consisted of 50 mM Tris-HCl, 0.2 mM EGTA, pH 7.4. Alkaline wash medium contained 2 mM EGTA adjusted to pH 12.0 using NaOH. Size-exclusion HPLC column buffer and sucrose gradient medium consisted of 150 mM NaCl, 5 mM MOPS, and 20 mM cholic acid, ±10 mM dithiothreitol, ±0.1% SDS, pH 7.2.

Tissue Culture. CHO-K1 cells were maintained in F12 medium (Ham, 1965) supplemented with 10% FBS, 100 units/mL penicillin, and 100 μg/mL streptomycin in a 37 °C humidified 5% CO_2 incubator.

Mutagenesis of GLUT1 cDNA. A 1.7 kbp *Bst*Y1 fragment of the human GLUT1 cDNA derived from pLENGT (Harrison et al., 1990a) was subcloned into the *Bam*HI cloning sites of M13mp19 (M13-GT1) and pGEM3Z (pGEM3Z-GT1). Oligonucleotide-directed point mutations were introduced by the modified phosphorothioate method of Eckstein (Nakamaye & Eckstein, 1986) using the Sculptor in vitro mutagenesis system. Each of the six cysteines in GLUT1 was mutagenized individually to serine using the following primers:

amino acid	primer
C133S	5′-CATCGGTGTGTAC**AG**CGGCCTG-3′
C201S	5′-CTGCTGCAG**AG**CA**TC**GTGCTGCCC-3′
C207S	5′-GCCCTTC**AG**CCCCGAGAG-3′
C347S	5′-ATGGCGG**GT**AGTGCCATACTCATG-3′
C421S	5′-GTGGGCATG**AG**CTTCCAGTATGTG-3′
C429S	5′-GAGCAACTGT**CT**GGTCCC-3′

where the underlined nucleotides are the codons targeted for mutagenesis. The nucleotide substitution is shown in boldface. Mutants were selected by sequencing M13 clones

[1] Abbreviations: GLUT1, erythrocyte glucose transporter; GLUT4, skeletal muscle glucose transporter; GLUT1-4C, chimeric glucose transporter consisting of GLUT1 residues 1−463 plus GLUT4 residues 480−509; GLUT1n-4, chimeric glucose transporter consisting of GLUT1 residues 1−199 plus GLUT4 residues 216−509; 2DODG, 2-deoxy-D-glucose; 3OMG, 3-*O*-methylglucose; C-Ab, anti-GLUT1 carboxy-terminal peptide antiserum; CCB, cytochalasin B; CHO, Chinese hamster ovary; ∂-Ab, anti-tetrameric GLUT1 rabbit antiserum; DABCO, 1,4-diazabicyclo[2.2.2]octane; DOTAP, *N*-[1-(2,3-dioleoyloxy)propyl]-*N*,*N*,*N*-trimethylammonium methylsulfate; DTT, dithiothreitol; EDTA, ethylenediaminetetraacetic acid; EGTA, ethylene glycol bis(β-aminoethyl ether)-*N*,*N*,*N*′,*N*′-tetraacetic acid; FBS, fetal bovine serum; GSH, glutathione; GSSG, oxidized glutathione; HEPES, *N*-(2-hydroxyethyl)piperazine-*N*′-2-ethanesulfonic acid; NTB, 2-nitro-5-thiobenzoic acid; NTSB, 2-nitro-5-thiosulfobenzoate; PAGE, polyacrylamide gel electrophoresis; SDS, sodium dodecyl sulfate; Tris-HCl, tris(hydroxymethyl)aminomethane hydrochloride; V8, endoproteinase glu-C.

across the following fragments which have unique restriction sites to facilitate subcloning:

amino acid	fragment
C133S	244 bp *HpaI/ApaI*
C201S, C207S	303 bp *ApaI/BstE2*
C347S	294 bp *BstE2/NheI*
C421S, C429S	461 bp *NheI/BamHI*

The fragment was excised from M13-GT1, subcloned into pGEM3Z-GT1, and resequenced across these restriction sites to verify the ligation region and the introduced mutation. Finally, wild-type and mutant cDNAs were subcloned into the pCMV5 expression vector (Anderson et al., 1989).

Stable Expression of Wild-Type and Mutant GLUT1 cDNAs in CHO-K1 Cells. Subconfluent CHO-K1 cells were cotransfected with GLUT1 cDNA and pRSVneo using the cationic lipid transfection reagent DOTAP (Leventis & Silvius, 1990). The transfected cells were grown in F12 media containing 250 μg/mL G418. G418-resistant cells were ring-cloned and expanded (Freshney, 1994). Clones expressing wild-type or mutant glucose transporters were identified by immunofluorescence and by Western blot analysis of total cellular membranes prepared as described previously (Harrison et al., 1990a) and blotted using C-Ab. CHO-cell plasma membranes and low-density microsomal membranes were isolated by homogenization and sucrose-cushion centrifugation exactly as described by Harrison et al. (1990b).

Red Cells and Red Cell Ghosts. Red cell ghosts were prepared from washed, intact red cells as described by Helgerson et al. (1989). Red cell ghosts were depleted of peripheral membrane proteins by a single wash in 5 volumes of alkaline wash medium (4 °C, 20 min). Membranes were collected by centrifugation (14000g for 5 min at 4 °C) and resuspended in 10 volumes of Tris medium. These membranes were subjected to three additional wash/centrifugation cycles in Tris medium, adjusted to 4 mg of membrane protein/mL, and stored at −70 °C.

Glucose Transport Protein. GLUT1 plus endogenous lipid was purified from human erythrocytes as described by Hebert and Carruthers (1992) or, in the presence of DTT, as described by Cairns et al. (1984).

ELISA. ELISA and competition ELISA were performed using C- and/or δ-Ab as described by Hebert and Carruthers (1992).

Nondenaturing Chromatography of GLUT1. Size-exclusion chromatography−HPLC (SEC−HPLC) studies of GLUT1-containing, cholate-solubilized membranes were performed using a Toso Haas TSK-Gel G4000 SWXL column as described previously (Hebert & Carruthers, 1992).

Cytochalasin B Binding Studies. Equilibrium, D-glucose (400 mM)-inhibitable [^{3}H]cytochalasin B binding to purified GLUT1 was determined as described previously (Hebert & Carruthers, 1992). Equilibrium cytochalasin B binding to red cells and red cell ghosts was measured as described in Helgerson and Carruthers (1987). Cytochalasin D (10 mM) was included in equilibrium cytochalasin B binding experiments to inhibit saturable cytochalasin B binding to non-glucose transporter sites (Jung & Rampal, 1977). DTT-containing cytochalasin B solutions were made freshly for each experiment since it was observed that prolonged exposure (>24 h) of cytochalasin B to DTT at −70 °C resulted in the irreversible loss of cytochalasin B binding to both nonreduced and reduced GLUT1.

Determination of GLUT1 Free Sulfhydryl and Disulfide Content. Both reduced and nonreduced, purified GLUT1 (each at approximately 100 μg/mL^{-1} in 1 mL and exhaustively dialyzed to remove traces of DTT) were denatured in 0.5% SDS in 50 mM Tris-HCl, 3 mM EDTA, pH 8.0, for 30 min. The solubilized protein was collected as supernatant by centrifugation (100000g for 1 h at 4 °C) and quantitated. The free sulfhydryl contents of reduced and nonreduced GLUT1 were determined by using Ellman's reagent (Rao & Scarborough, 1990). The reaction was initiated by addition of 100 μL of freshly prepared 10 mM 5,5′-dithiobis-(2-nitrobenzoic acid) (DTNB). The course of the reaction at room temperature was recorded as the increase in absorbance at 412 nm. GLUT1 disulfide content was measured by the 2-nitro-5-thiosulfobenzoate (NTSB) assay in which disulfides are cleaved by sulfitolysis and the resulting free sulfhydryls quantitated (Rao & Scarborough, 1990). An extinction coefficient of 13 600 M^{-1} cm^{-1} at 412 nm for 2-nitro-5-thiobenzoic acid (NTB) was used to quantitate both reactions. All NTSB assays included the parallel, internal controls of porcine insulin (three disulfides per molecule) and oxidized glutathione (one disulfide per molecule).

GLUT1 Alkylation/Proteolysis. The procedure of Rao and Scarborough (1990) was used to label either all cysteine residues or free cysteine residues of GLUT1 purified in the absence of DTT. Briefly, GLUT1 (1 mg/mL) was unfolded in SDS, reduced (or not reduced), and alkylated using 0.6 mM [^{14}C]iodoacetic acid (incubation was in 0.2 M Tris-HCl, 2 mM EDTA, and 1% SDS, pH 8.3, for 25 min at room temperature in the dark). Alkylation was terminated by addition of 2-mercaptoethanol (0.5%; 64 mM), and free label was removed by extensive dialysis. Labeled GLUT1 was electrophoresed on a preparative urea−acrylamide gel in the dark. This gel consisted of 9 M urea, 11% acrylamide, 375 mM Tris-HCl, pH 8.8, and 0.2% SDS. Samples were solubilized in an equal volume of sample buffer and electrophoresed at 3 W constant power. Gels were rinsed for 20 min in deionized water to remove urea and then vacuum-dried. Dried gels were exposed overnight to X-ray film to locate the radiolabeled GLUT1.

Peptide mapping of labeled GLUT1 peptides was performed either as described previously (Carruthers & Helgerson, 1989) or with the following modifications. Pieces of dried gel (5 × 8 mm) were excised from the preparative gel and inserted into wells of a stacking gel containing sample buffer and 8 μg of V8 protease. The dried gel piece was allowed to soak up the buffer, and running buffer was then used to cover the well. Samples were electrophoresed into the stacking gel, and the power was interrupted for 1 h to allow proteolytic digestion of GLUT1. Power was resumed, and the peptides were allowed to separate in the 18% gel. Electrophoresis was performed in the dark. Peptides were then transferred to Immobilon-P membrane filters for immunoblot analysis or for staining with Coomassie Brilliant Blue R and subsequent sequence analysis. When peptides were isolated in this manner for N-terminal sequence analysis, acrylamide gels were pre-run and were electrophoresed in the presence of 1 mM thioglycolate. Parallel lanes were also run for visualization of alkylated peptides by autoradiography.

3-O-Methylglucose Uptake by Erythrocytes. 3-*O*-Methylglucose uptake was measured as described previously (Helgerson et al., 1989). Briefly, sugar-free red cells (at ice

temperature) were exposed to 5 volumes of saline (ice temperature) containing variable [30MG] and fixed [[^{3}H]-30MG]. Uptake was permitted to proceed for 10−30 s, and then 50 volumes (relative to the cell volume) of stopper solution was added to the cell suspension. Cells were sedimented by centrifugation (14000g for 15 s at 4 °C), washed once in stopper, collected by centrifugation (14000g for 15 s at 4 °C), and extracted in 1 mL of 3% perchloric acid. The acid extract was centrifuged (14000g for 15 s at 4 °C), and duplicate samples of the clear supernatant fluid were counted. Zero-time uptake points were prepared by addition of stopper to cells prior to addition of medium containing sugar and radiolabel. Cells were immediately processed. Radioactivity associated with cells at zero-time was subtracted from the activity associated with cells following the uptake period. All uptakes were normalized to equilibrium uptake where cells were exposed to sugar medium at 37 °C for 30 min prior to addition of stopper. This procedure limits the experimental 30MG space of the cells to 10% or lower. CHO cell 2-deoxy-D-glucose uptake was measured at 22 °C, in 24-well dishes using 100 μM 2-deoxy-D-glucose as described previously (Harrison et al., 1990a). 3-*O*-Methylglucose exit from erythrocytes was measured as described by Helgerson and Carruthers (1989).

Calculation of Transport and Ligand Binding Parameters. V_{max} and $K_{m(app)}$ for 30MG uptake were computed by direct, nonlinear regression analysis of the concentration dependence of 30MG uptake assuming Michaelis−Menten kinetics. $K_{d(app)}$ and B_{max} for cytochalasin B binding to GLUT1 were computed by direct, nonlinear regression analysis of the concentration dependence of cytochalasin B binding assuming binding is described by simple saturation kinetics. The software package used was KaleidaGraph 3.0 (Synergy Software, Reading, PA).

Immunofluorescence Microscopy of Cells. For red blood cells, circular coverslips were washed in 70% ethanol, 1% HCl for 1 h, oven-dried, immersed in a 10% solution of polylysine for 5 min, and then air-dried overnight. Washed erythrocytes (10 μL, 50% hematocrit) were pipetted onto polylysine-coated coverslips positioned above 5 mL of saline in 50 mL Falcon tubes. These tubes were then centrifuged at 1100g for 5 min, and unattached cells were removed by addition and subsequent aspiration of saline (20 mL). Two additional saline washes were made; then the erythrocyte-coated coverslips were transferred to 6 well tissue culture dishes for immunohistochemical processing.

Antibody binding to cells was measured in cells that were either unfixed or fixed and permeabilized. Fixation was for 15 min in saline containing 4% paraformaldehyde followed by two washes in saline containing 1% fetal bovine serum. Fixed cells were permeabilized by 15 min incubation at room temperature in saline containing 0.05% Triton X-100 and 1% FBS followed by four washes in saline containing 1% FBS. Fixed and unfixed cells were then incubated for 60 min in saline containing 1% FBS plus C-Ab (1:5000 dilution of crude serum) and/or plus δ-Ab (1:5000 dilution of crude serum). Cells were washed 3 times in FBS saline and then incubated for 30 min with rhodamine-conjugated goat anti-rabbit (anti-C-Ab) IgGs (4 μg/mL) or with fluorescein-conjugated rabbit anti-sheep (anti-δ-Ab) IgGs (4 μg/mL). In experiments where both C-Ab binding and δ-Ab binding were measured simultaneously, cells were subsequently exposed to rhodamine-conjugated goat anti-rabbit (anti-CAb) IgGs followed by washing and exposure to fluorescein-conjugated rabbit anti-sheep (anti-δ-Ab) IgGs. Cells were then washed 3 times in saline, the coverslips mounted on a slide with 2.5% DABCO (Sigma Chemicals), 90% glycerol, and the slides sealed with clear nail polish.

CHO cell lines were plated directly onto sterile coverslips in 6 well plates 48 h prior to processing. Cells were washed 3 times with PBS and fixed for 15 min at room temperature with 2% paraformaldehyde in PBS with or without preincubation in 5 mM DTT for 15 min at room temperature. Subsequent washes were done with PBS plus 1% FBS. After being fixed, cells were solubilized with 0.05% Triton X-100 for 15 min at room temperature. Fixed, solubilized cells were then incubated for 1 h at room temperature with PBS containing 1% FBS, rabbit C-Ab (1:5000 dilution of crude serum), and/or sheep δ-Ab (1:5000 dilution of crude serum). The cells were washed and incubated for 30 min at room temperature in PBS containing 1% FBS, goat anti-rabbit IgG−Rhodamine (4 μg/mL dilution), and then for 30 min at room temperature in PBS containing 1% FBS, rabbit anti-sheep IgG−FITC (4 μg/mL). The coverslips were washed extensively, mounted in 90% glycerol, 2.5% DABCO, and sealed with clear nail polish.

Samples were visualized by fluorescence microscopy using a Nikon Diaphot 200 microscope with a Nikon Apo 60/1.4 oil immersion lens. Images were digitized with 14-bit resolution using a thermoelectrically cooled CCD camera (Photometrics Ltd., Tuscon, AZ) and stored on magnetic media for subsequent analysis.

Analytical Procedures. Protein was determined by the Pierce BCA procedure (Brown et al., 1989). SDS-slab (10 or 18%) PAGE of membrane proteins and GLUT1 was as described previously (Carruthers & Helgerson, 1989). Immuno- (Western) blotting of proteins using δ- or C-Ab was as described in Harrison et al. (1990a). Immune serum (δ-Ab) specific [^{125}I]protein A binding to erythrocyte membranes was determined as described previously (Harrison et al., 1990a). Amino acid and N-terminal sequence analysis of Immobilon membrane-bound peptides was performed by Dr. John Leszyk, Director of the Core Laboratory for Protein Chemistry at the Worcester Foundation for Experimental Biology, Shrewsbury, MA. Densitometric analysis of autoradiograms was carried out either by using a Hoefer GS300 Transmittance/Reflectance Scanning Densitometer in combination with the GS-370 data system (Apple Macintosh Version) or by using the software package NIH Image (v 1.5.7, National Institutes of Health) to analyze autoradiograms digitized at 8-bit resolution.

RESULTS

GLUT1 Sulfhydryl Chemistry. The purified GLUT1 preparation contains red cell lipid (Hebert & Carruthers, 1991), GLUT1 [$M_{r(app)}$ = 55K; Figure 1, lanes 2 and 3], and red cell band 7 or RhD protein [$M_{r(app)}$ = 33K, peptide a of Figure 1, lanes 2 and 3]. Amino acid composition analyses of these proteins following electrophoretic transfer to Immobilon membranes indicate that the molar ratio of GLUT1 to band 7 present in the GLUT1 preparation is 1:0.04. This is consistent with our frequent but qualitative observation that GLUT1 is stained very poorly by Coomassie.

SDS-unfolded, nonreduced, purified GLUT1 exposes two thiol groups per GLUT1 monomer (Table 1) and is resolved as a monomer during nonreducing SDS−PAGE (Figure 1, lanes 2 and 3). Reduced GLUT1 exposes six sulfhydryl groups per GLUT1 monomer (Table 1). Because the

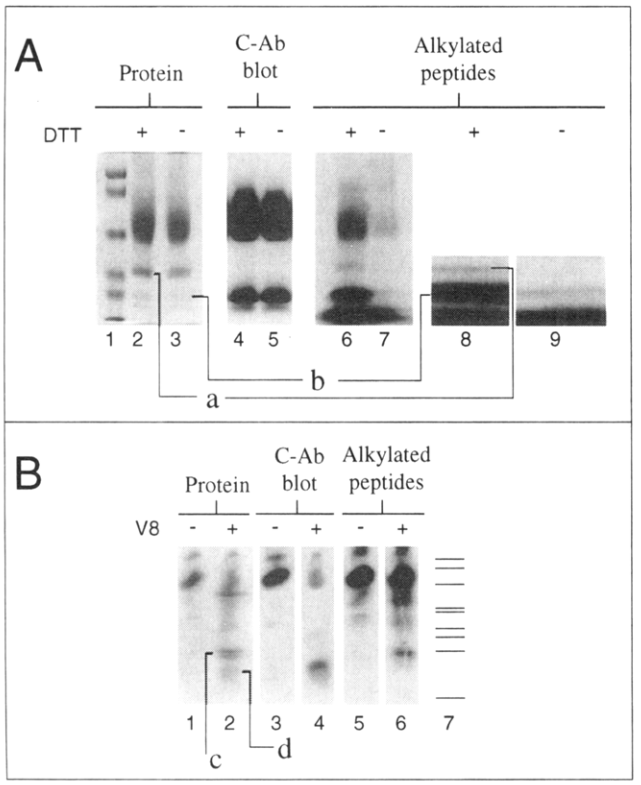

FIGURE 1: (A) Analysis of tryptic fragments of differentially alkylated GLUT1. Molecular mass markers are shown in lane 1. These are (in order of decreasing molecular mass) 106.5, 80, 49.5, 32.5, 27.5, and 18.5 kDa. Coomassie-stained protein is shown in lanes 2 and 3. Peptides with intact C-termini (C-Ab-reactive peptides) are shown in lanes 4 and 5. [^{14}C]Iodoacetic acid-labeled peptides are shown in lanes 6 through 9. Lanes 8 and 9 are sections of single-lane gels used to purify peptides for N-terminal sequence analysis. In lanes 2−5, nonreduced, tetrameric GLUT1 was subjected to reducing (DTT+) or nonreducing (DTT−) SDS−PAGE. In lanes 6, 7, 8, and 9, nonreduced GLUT1 was either reduced (DTT+) or nonreduced (DTT−) prior to alkylation and reducing SDS−PAGE. Peptide a is Band 7 or RhD (see Results). The identity of peptide b is shown in Table 1. (B) V8 peptide mapping of urea−gel electrophoresis purified, alkylated tetrameric GLUT1. Lanes 1 and 2 show Coomassie-stained protein. Lanes 3 and 4 show peptides containing intact C-termini as judged by immunoblot analysis using anti-GLUT1 carboxyl-terminal peptide antiserum (C-Ab). Lanes 5 and 6 are 2-week autoradiographic exposures of alkylated GLUT1 and show [^{14}C]iodoacetic acid incorporation. Lane 7 shows the mobility of molecular mass markers. These are (in order of decreasing molecular mass) 139.9, 86.8, 47.8, 33.3, 26.6, 20.4, 16.9, 14.4, and 6.2 kDa. Exposure to (+) or omission of (−) V8 protease is indicated above the lanes. Peptides c and d were subjected to N-terminal sequence analysis. Their identities are shown in Table 1.

deduced cysteine content of GLUT1 is six residues per polypeptide (Mueckler et al., 1985), this raises the possibility each GLUT1 molecule contains as many as two intramolecular disulfide bridges. We assayed nonreduced GLUT1 disulfide content by using the 2-nitro-5-thiosulfobenzoate (NTSB) assay in which disulfides are cleaved by sulfitolysis and the resulting free sulfhydryls are quantitated by measuring the release of nitro-5-thiobenzoate (Rao & Scarborough, 1990). Sulfitolysis of SDS-unfolded tetrameric GLUT1 disulfides reveals an additional 3 mol of reactive sulfhydryl groups per mole of GLUT1 (Table 1).

Table 1 summarizes the results of three types of alkylation strategies in which free sulfhydryls, inaccessible sulfhydryls, and all sulfhydryl groups are labeled using [^{14}C]iodoacetic acid. Inaccessible sulfhydryl groups are revealed by first alkylating nonreduced GLUT1 with unlabeled ([^{12}C]-) iodoacetic acid; then GLUT1 is reduced and alkylated using [^{14}C]iodoacetic acid. Reduced GLUT1 incorporates almost 3 times more [^{14}C]iodoacetic acid than does nonreduced GLUT1. Differential alkylation of unavailable sulfhydryl groups in nonreduced GLUT1 results in almost 2-fold greater [^{14}C]iodoacetic acid labeling relative to [^{14}C]iodoacetic acid labeling of available sites. Since these data and quantitation of GLUT1 sulfhydryls using Ellman's reagent show that GLUT1 exposes all six potential thiols following exposure to reductant, the results of the NTSB assay are consistent with the view that each GLUT1 molecule contains one intramolecular disulfide bridge and either two mixed disulfides or two free thiols that are exposed only upon reduction of the internal disulfide bridge.

One GLUT1 cysteine residue occurs within a proposed cytosolic GLUT1 domain, four lie in proposed transmembrane domains, and the remaining residue is predicted to contact the interstitium (Mueckler et al., 1985). To determine which GLUT1 cysteines are inaccessible in tetrameric GLUT1, we subjected alkylated GLUT1 to proteolysis and N-terminal sequence analysis. Reduced GLUT1 and nonreduced GLUT1 were alkylated and mildly trypsinized, and the resulting peptides were separated by SDS−PAGE under reducing or nonreducing conditions. Total peptides were detected by staining, alkylated peptides were detected by autoradiography, and peptides containing an intact C-terminus were detected by immunoblot analysis using anti-GLUT1 carboxyl-terminal peptide antiserum (C-Ab). Peptides detected by all three criteria were subjected to N-terminal sequence analysis. Figure 1A (lanes 6, 7) shows that reduced intact GLUT1 is alkylated 4-fold more heavily than is nonreduced intact GLUT1. Lanes 6−9 of the same figure also show that a peptide of apparent molecular mass 25 kDa (peptide b) is heavily labeled by iodoacetic acid when the transporter is reduced prior to alkylation and proteolysis. This peptide cross-reacts with C-Ab, and neither its mobility nor its yield is affected significantly by omission of reductant during electrophoresis.

Quantitation of label incorporation indicates that the 25 kDa peptide incorporates 99 and 8 pmol of iodoacetic acid/μg of peptide when labeled after or before reduction, respectively. By contrast, GLUT1 incorporates 117 and 33 pmol of iodoacetic acid/μg of GLUT1 when labeled after or before reduction, respectively. N-Terminal sequence analysis by Edman degradation indicates that the N-terminus of the 25 kDa peptide is $_{233}$GTADVTHDLQEMKEE$_{247}$.

Since this peptide also contains an intact C-terminus, this allows a peptide assignment of GLUT1 residues 233−(480−492). The last 13 residues are less certain since the polyclonal, GLUT1 C-terminal peptide antiserum is raised against GLUT1 residues 480−492 and may not bind to all 13 residues. Assuming all 13 C-terminal residues are present, this peptide has a deduced molecular weight of 28 705. Iodoacetic acid incorporation into this peptide is thus 2.8 and 0.2 mol/mol of reduced and nonreduced peptide, respectively.

The other low molecular mass protein present in the GLUT1 preparation (peptide a of Figure 1A) has a computed molecular mass of 33 kDa. This peptide does not react with C-Ab and is labeled only very weakly by iodoacetic acid. The N-terminal sequence derived for this peptide is SSKYPRSVRR, which corresponds to N-terminal residues 2−11 of RhD, a component of Band 7 protein in human erythrocytes (Arce et al., 1993).

Table 1: Sulfhydryl Chemistry of GLUT1

		mol of [^{14}C]iodoacetic acid incorporated/mol of protein or peptide	mol of SH/ mol of GLUT1[a]	NTSB assay[b] (mol of NTB/mol of GLUT1)
tetrameric GLUT1	nonreduced	1.8 ± 0.2	2.2 ± 0.1	4.8 ± 0.3
	reduced	6.4 ± 0.1	6.7 ± 0.4	
	^{12}C-alkylated, then reduced[c]	3.8 ± 0.3		
	^{12}C-alkylated[c]	0.1 ± 0.1		
peptide, N-terminal sequence, and deduced residues				
b, GTADVTHDLQEMKEE (233−492)	nonreduced	0.2		
b, GTADVTHDLQEMKEE (233−492)	reduced	2.8		
c, VSPTALRGALGT (147−298)	nonreduced	1.7		
d, SRQMMREKKV (248−358)	nonreduced	<0.1		
d, KAGVQQPVYA (300−425)	nonreduced	<0.1		
d, VGPGPIPWFI (381−492)	nonreduced	<0.1		
d, LFSQGPRPAA (394−492)	nonreduced	<0.1		
dimeric GLUT1	reduced		6.2 ± 0.2	

[a] GLUT1 free sulfhydryl content was assayed using Ellman's reagent. [b] GLUT1 disulfides were cleaved using sulfitolysis and the exposed thiol groups quantitated using NTSB. [c] ^{12}C-Alkylated protein was treated with cold (unlabeled) iodoacetic acid prior to treatment with [^{14}C]iodoacetic acid. Peptides identified as **b**, **c**, and **d** are those indicated in Figure 1. Assays of GLUT1 sulfhydryl content and disulfide bond content were made in duplicate on at least three separate occasions.

Nonreduced, alkylated GLUT1 was also subjected to urea gel electrophoresis. Intact GLUT1 was identified by immunoblot analysis, excised from the gel, and subjected to Cleland mapping using V8 protease. Peptides were transferred to Immobilon and subjected to N-terminal sequence analysis. Figure 1B (lanes 2 and 6) shows that a peptide of $M_{r(app)}$ 15K (peptide c) is heavily alkylated. The N-terminal sequence of this fragment is $_{147}$VSPTALRGALGT$_{156}$.

Quantitation of iodoacetic acid incorporation indicates 113 pmol of reactive thiols/μg of peptide. Figure 1B (lanes 2, 4, and 6) also shows that a peptide(s) of $M_{r(app)}$ 11.6K (peptide d) cross-react(s) with C-Ab on immunoblot analysis but is (are) not alkylated appreciably. Sequence analysis indicates that this region of the blot contains as many as four peptides with N-terminal sequences $_{248}$SRQMMREKKV$_{257}$, $_{300}$KAGVQQPVYA$_{309}$, $_{381}$VGPGPIPWFI$_{390}$, and $_{394}$LFSQGPRPAA$_{403}$.

Each of these peptides falls within the C-terminal domain of tetrameric GLUT1 (residues 233−492) that lacks accessible thiol groups. If two of these peptides were to contain an intact GLUT1 C-terminus (i.e., GLUT1 peptides 381−492 and 394−492), they would be characterized by a predicted M_r of 12.3K and 11K, respectively, and could account for C-Ab binding to this region of the blot.

Mutagenesis of GLUT1 Cysteines. GLUT1 cysteines were mutagenized to serines by oligonucleotide-directed *in vitro* mutagenesis. The resulting cDNAs were subcloned into pCMV5 expression vectors for CHO cell transfection. CHO cells were chosen for GLUT1 expression because sugar transport by both CHO cells and erythrocytes is inhibited by extracellular reductant (see below). This suggests that erythrocytes and CHO cells process GLUT1 in a similar fashion.

Clonal cell lines expressing GLUT1 wild-type and cysteine mutants were screened for the extent of GLUT1 overexpression by immunoblot analysis and by immunofluorescence microscopy. Two antisera were used. δ-Ab binds to exofacial epitopes of native, tetrameric GLUT1 but fails to react with dimeric GLUT1 (Hebert & Carruthers, 1992) while C-Ab binds to the intracellular C-termini of both tetrameric and dimeric GLUT1 (Hebert & Carruthers, 1992).

Immunoblot analyses of CHO cell total membranes using C-Ab indicate that clonal cells express wild-type or mutant glucose transporter at levels 2−4-fold greater than levels of GLUT1 expression in parental CHO-K1 cells (Table 2). CHO cell total membranes were also subfractionated into plasma membrane and low-density microsomal membrane fractions. In two separate experiments where all GLUT1 cysteine mutants were examined, the ratio of plasma membrane GLUT1 content (protein detected by immunoblot analysis of 100 μg of membrane total protein) to low-density microsomal membrane GLUT1 content (1:0.5) was unaltered by mutagenesis of GLUT1 cysteine residues to serines. This suggests that cellular processing of GLUT1 is unaffected by serine substitution of cysteine.

Total GLUT1 expression was also quantitated by digital imaging fluorescence microscopy (DIFM) using C-Ab. Since C-Ab does not bind to intact cells, this requires that fixed cells are first permeabilized either by using nonionic detergent (e.g., 0.05% Triton X-100) or by using paraformaldehyde levels in excess of 2% (w/v) during fixation. Immunofluorescence quantitation was by three methods. Total, specific immunofluorescence from the field was quantitated and divided by the number of cells in the field. In the second approach, specific immunofluorescence of individual cells was quantitated and averaged over a large number of cells. These methods can suffer from the depth of field phenomena (see below) so a third approach was used in which specific immunofluorescence within patches of flattened cellular extensions was measured. The results of all three approaches are in close agreement. The C-Ab immunofluorescence data of Table 2 are computed using the specific, cellular immunofluorescence approach and are not significantly different (two-tailed paired t-test) from the results of immunoblot analyses using C-Ab (Table 2).

The depth of field phenomenon is illustrated by the fluorescence micrographs of the C347S mutant in Figure 2. For one cell in the field of view, both C-Ab and δ-Ab staining patterns suggest an unusual, local sequestration of the mutant protein. The second cell in the same field does not show this behavior. In fact, this local fluorescence intensity is a cell-shape phenomenon. In this hot spot, the value for the z-axis is large (reflecting cell morphology), and the light intensity collected from a given area of x y-pixels reflects the magnitude of the z-plane (Agard et al., 1989). Total cellular fluorescence is relatively constant. This phenomenon

Table 2: GLUT1 Expression in CHO Cells

cell type	immunoblot[a]	immunofluorescence microscopy[b]		
	C-Ab	δ-Ab[b]	C-Ab[b]	δ-Ab/C-Ab[c]
CHO-K1[d]	1	1	1	1
CWT	3.4 ± 0.7	4.8 ± 1.3	3.7 ± 0.8	1.3 ± 0.1 (0.4)
C133S	2.4 ± 0.2	7.9 ± 4.5	5.0 ± 2.2	1.3 ± 0.2 (0.7)
C201S	2.9 ± 0.2	5.4 ± 1.7	3.6 ± 0.8	1.4 ± 0.3 (1.2)
C207S	3.3 ± 0.6	7.1 ± 3.5	5.4 ± 2.4	1.2 ± 0.1 (0.3)
C347S	2.8 ± 0.4	0.9 ± 0.2[e,f]	4.9 ± 1.6	0.3 ± 0.1 (0.4)[g]
C421S	3.1 ± 0.6	0.9 ± 0.2[e,f]	4.5 ± 1.4	0.3 ± 0.1 (0.4)[g]
C429S	2.9 ± 0.4	5.3 ± 2.3	3.6 ± 1.0	1.3 ± 0.2 (0.8)
GT3[h]	9.3 ± 0.6	8.0 ± 1.0	7.2 ± 1.8	1.2 ± 0.2 (0.6)
GLUT1-4C[i]	1	5.5 ± 1.6[j]	2.0 ± 0.9	3.4 ± 1.1 (3.5)
GLUT1n-4[i]	1	1.9 ± 0.2	0.8 ± 0.3	3.1 ± 1.5 (4.9)

[a] Intact GLUT1 was quantitated by immunoblot analysis of 100 μg of CHO cell membrane protein using C-Ab as the primary antiserum and [^{125}I]protein A as the reporter molecule. Resulting autoradiograms were quantitated by densitometry. [b] δ-Ab and C-Ab binding to fixed permeabilized CHO cells was measured simultaneously by digital imaging fluorescence microscopy using fluorescein-conjugated rabbit anti-sheep IgGs as the reporter molecule for δ-Ab binding and rhodamine-conjugated goat anti-rabbit IgGs as the reporter molecule for C-Ab binding. [c] The ratio of cellular δ-Ab binding (fluorescein fluorescence) to C-Ab binding (rhodamine fluorescence) was computed for each cell analyzed. The numbers in parentheses indicate the range of results. [d] All results are expressed relative to those obtained with CHO-K1 parental cells within the same experiment. The following summarizes unadjusted data for CHO-K1 cells: immunoblot analysis, 59 701 ± 10 121 arbitrary units per 100 μg of membrane protein; δ-Ab binding, (3.2 ± 0.37) × 10^6 arbitrary fluorescence units per cell; C-Ab binding, (1.06 ± 0.19) × 10^6 arbitrary fluorescence units per cell; δ:C ratio, (3.19 ± 0.20):1. All results are significantly greater than those obtained with control, CHO-K1 cells ($p < 0.05$; 1-tailed paired *t*-test) with the exception of [e] in which these results are not significantly different from control and [g] in which the result is significantly lower than control ($p < 0.005$; 1-tailed paired *t*-test). No significant statistical differences exist across columns 2 through 4 with the exception of [f] in which this result is significantly less ($p < 0.05$; 1-tailed paired *t*-test) than those obtained by immunoblot or immunofluorescence analysis using C-Ab and [j] in which this result is significantly greater ($p < 0.05$; 1-tailed paired *t*-test) than that obtained by immunofluorescence analysis using C-Ab. [h] GT3 cells are the CHO cell line that expresses GLUT1 at very high levels (Harrison et al., 1990a). [i] Immunoblot data for GLUT1-4C and GLUT1n-4 are taken from Pessino et al. (1991). Results are shown as mean ± SEM of three or more separate determinations.

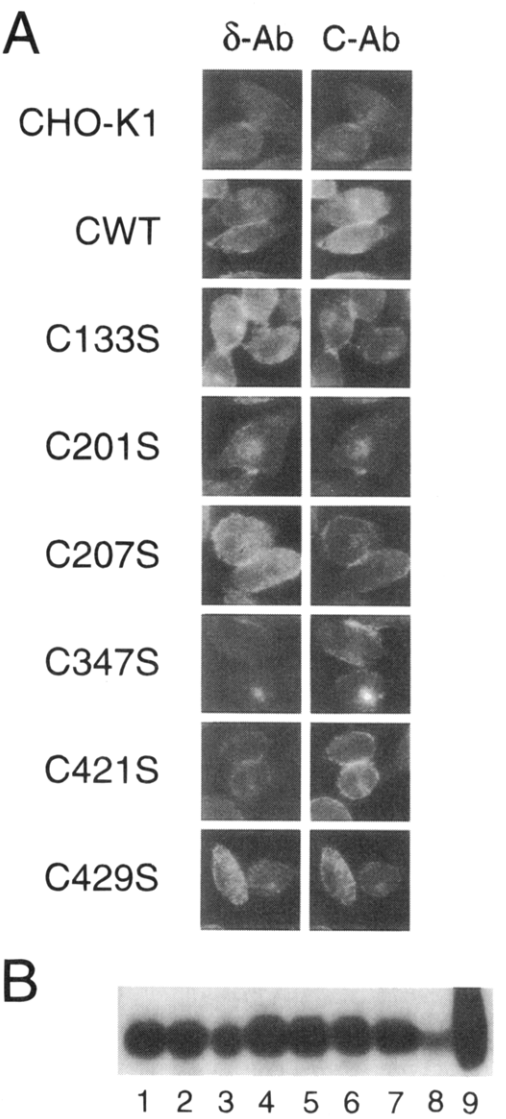

FIGURE 2: (A) Cells were fixed, permeabilized, and stained for δ-Ab- and C-Ab-reactive epitopes. Fluorescein- and rhodamine-conjugated secondary antibodies were used. Results are shown for parental CHO-K1 cells, for a wild type GLUT1 overexpresser (CWT), and for cysteine mutants 133, 201, 207, 347, 421, and 429 (C133S through C429S). For display purposes, the full range of fluorescence intensities associated with all images acquired using a given primary antiserum is compressed to a scale of 0−255 (8-bit resolution). This aids visual comparison of the range of staining intensities obtained with different cells but using one antiserum. For example, CWT express δ-Ab-reactive epitopes at levels 3-fold greater than do CHO-K1 parental. The actual (measured) range of fluorescence intensities in this experiment is 0−4753 (arbitrary units) for δ-Ab binding images and 0−2953 for C-Ab binding images. (B) Immunoblot analysis (using C-Ab as primary antiserum) of cell membranes (100 μg of total membrane protein) from cells of panel A. The blots are wild-type expresser (CWT, lane 1); GLUT1 cysteine mutants C133S, C201S, C207S, C347S, C421S, and C429S (lanes 2−7, respectively); and CHO-K1 cells (lane 8). Lane 9 contains 250 ng of purified GLUT1.

was observed infrequently in all clonal cell lines and was most common when cells were characterized by a rounded morphology.

Since transfected CHO cells express GLUT1 Cys mutants, we next determined whether these cells also expose increased levels of tetrameric GLUT1-specific (δ -Ab binding) epitopes. These data were collected from the same cells that were analyzed for GLUT1 expression levels by C-Ab fluorescence. This is possible because these cells were dual-labeled for both C-Ab- and δ-Ab-reactive epitopes. Cells were fixed, permeabilized, and exposed to sheep δ-Ab and rabbit C-Ab. C-Ab binding was detected by using rhodamine-conjugated goat anti-rabbit IgGs. The cells were washed, and δ-Ab binding was detected by using fluorescein-conjugated rabbit anti-sheep IgGs. As with quantitation of C-Ab binding, δ-Ab binding was quantitated using the specific individual cellular immunofluorescence approach. In three separate experiments, we also stained cells separately for δ-Ab and for C-Ab binding and obtained results indistinguishable from those obtained by the simultaneous staining procedure.

The data we collected are expressed in two ways. Specific (δ-Ab or C-Ab) cellular immunofluorescence is expressed relative to that measured in CHO-K1 parental cells. For example, Table 2 shows that the C429S GLUT1 mutant expresses δ-Ab and C-Ab reactive sites at levels 5.3- and 3.6-fold greater, respectively, than do CHO-K1 cells. Figure 2 shows typical immunofluorescence micrographs where C429S GLUT1 expressing CHO cells show approximately 4-fold greater δ-Ab and C-Ab staining than do CHO-K1 cells.

The ratio of δ-Ab to C-Ab staining in a given cell for a given experiment is also computed and is expressed relative to this same ratio in CHO-K1 cells. This facilitates comparison of GLUT1 cysteine mutant δ-Ab and C-Ab

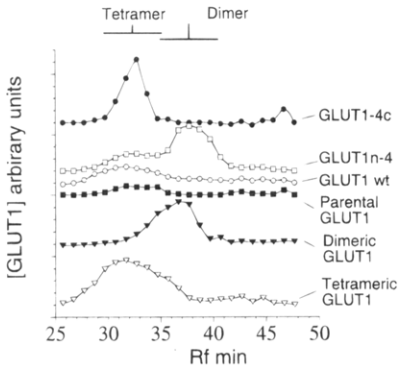

FIGURE 3: Hydrodynamic size analysis of GLUT1/GLUT4 chimeras. Cell membranes from parental CHO cells (■) and from CHO cells expressing wt GLUT1 (○), GLUT1n-4 (□), or GLUT1-4c (●) (Pessino et al., 1991) were solubilized in cholate and applied to a size-exclusion column as in Hebert and Carruthers (1992). Chimeras and GLUT1 were detected by ELISA using anti-GLUT4- or anti-GLUT1-C-terminal peptide antisera, respectively. Authentic tetrameric (▽) and dimeric (▼) GLUT1 are also shown.

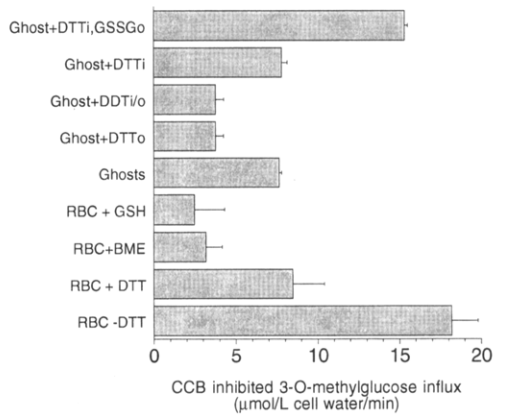

FIGURE 4: 3-*O*-Methylglucose uptake (66 μM sugar, 4 °C) by erythrocytes (RBCs) in the presence or absence of 2 mM extracellular reductants (glutathione, dithiothreitol, and β-mercaptoethanol) and by erythrocyte ghosts (ghosts) containing (e.g., DTT_i) or lacking 2 mM reductant and exposed to 2 mM extracellular reductants (e.g., DTT_o) or 2 mM oxidized glutathione. Results represent the mean ± SEM of at least four separate experiments made in triplicate.

binding properties with those of GLUT1 in a cell (CHO-K1) where almost all GLUT1 forms a homotetratrameric structure [e.g., see Hebert and Carruthers (1992) and see Figure 3]. The δ-Ab:C-Ab binding ratio is not, however, a direct measure of the absolute ratio of cellular tetrameric GLUT1 to total cellular GLUT1. The δ-Ab:C-Ab binding ratio also provides an internal control for individual experiments. Thus, while variations in levels of cellular expression of GLUT1 and GLUT1 cysteine mutants exist between experiments and are evident from standard errors computed in columns 2−4 of Table 2, the ratio of cellular δ-Ab to C-Ab binding sites (for δ-Ab binding competent GLUT1) is much less variable because this ratio is independent of GLUT1 expression level.

The results (summarized in Figure 2 and Table 2) show that serine substitution at cysteine 347 or 421 significantly reduces GLUT1 exposure of tetrameric GLUT1-specific epitopes. Some variation between experiments is observed, and ranges for δ-Ab:C-Ab binding ratios are provided in Table 2.

Mapping Oligomerization Domains. We have previously shown that specific immunoprecipitation of GLUT1−GLUT4 chimeras expressed in CHO cells by using anti-GLUT4 antiserum results in coimmunoprecipitation of endogenous GLUT1 protein (Pessino et al., 1991). The transporter chimeras used in these studies were GLUT1-4c (GLUT1 residues 1−463 plus the 30 C-terminal residues of GLUT4) and GLUT1n-4 (GLUT1 residues 1−199 plus the 294 C-terminal residues of GLUT4). Since coimmunoprecipitation of 3T3L1 adipocyte GLUT4 and GLUT1 is not observed under the same conditions, we concluded that GLUT1-specific domains mediate GLUT1/chimera associations (Pessino et al., 1991).

We have now determined the hydrodynamic radius of glucose transporter-containing micelles solubilized from these cells. Our analyses (Figure 3) indicate that parental GLUT1, wtGLUT1, GLUT1−4c, and 25% of expressed GLUT1n-4 coresolve with authentic tetrameric GLUT1 upon size-exclusion chromatography. The majority of GLUT1n-4, however, coresolves with authentic dimeric GLUT1.

GLUT1 Structure, GLUT1-Mediated Sugar Transport, and Ligand Binding in Intact Cells. GLUT1-mediated 3-*O*-methylglucose uptake by human erythrocytes is inhibited 3−15-fold by dithiothreitol, by 2-mercaptoethanol, and by reduced glutathione preincubation at 37 °C (Figure 4) while oxidized glutathione stimulates red cell sugar import (Figure 4). The inhibitory action of dithiothreitol is noncompetitive (Table 3) and is half-maximal at 0.7 ± 0.1 mM (SEM of four experiments). This effect is exerted at the exofacial surface of the cell membrane since glutathione and oxidized glutathione are cell-impermeable (Kondo et al., 1989; Srivastava & Beutler, 1969). Removal of extracellular DTT from 2 mM DTT-loaded ghosts results in reversal of transport inhibition but does not deplete ghosts of intracellular reductant as judged by quantitation of the release of DTNB-reactive species upon addition of Triton X-100. 3-*O*-Methylglucose exist is unchanged in DTT-exposed cells shown in parallel experiments to have reduced sugar uptake ($n = 3$).

Cytochalasin B binding to red cells and to resealed, hemoglobin-depleted red cell ghosts is affected by DTT in two ways: (1) Sugar-inhibitable cytochalasin B binding capacity is increased 2.4-fold following red cell incubation with 2 mM DTT (Table 3). (2) The kinetics of maltose inhibition of cytochalasin B binding are converted from

Table 3: Effects of Reductant on GLUT1 Function

parameter	control	DTT
v_{max}[a]	276 ± 28	138 ± 32
$K_{m(app)}$[a]	0.11 ± 0.08	0.18 ± 0.05
B_m[b]	128 ± 16	315 ± 22
$K_{d(app)}$[b]	91 ± 8	137 ± 16
CHO-K1 cells[c]	167 ± 11	77 ± 4
CWT cells[c]	275 ± 14	131 ± 9

[a] V_{max} is the maximum velocity (micromoles per liter of cell water per minute) and $K_{m(app)}$ the Michaelis constant (millimolar) for 3-*O*-methylglucose uptake by control and DTT (2 mM)-treated erythrocytes at 4 °C. Results represent the mean ± SEM of three separate experiments made in triplicate. [b] B_m and $K_{d(app)}$ represent the maximum binding capacity (thousands of sites per cell) and dissociation constant (nanomolar) for equilibrium cytochalasin B binding to erythrocytes. Results represent the mean ± SEM of five separate experiments made in triplicate. [c] CHO-K1 and CWT cell experiments measure cytochalasin B (20 μM)-inhibitable 2-deoxy-D-glucose uptake (micromoles of sugar per liter of cell water per minute) by parental and GLUT1-transfected CHO cells at 100 μM sugar and 22 °C. Results are shown as mean ± SEM of three separate experiments measured in quintuplicate. The water (3-*O*-methylglucose) space of a single CHO cell is 0.98 pL. CHO-K1 cell uptake and CWT cell 2-deoxy-D-glucose uptake in the presence of 20 μM cytochalasin B are 53 and 46 μM (L of cell water)$^{-1}$ min^{-1}, respectively.

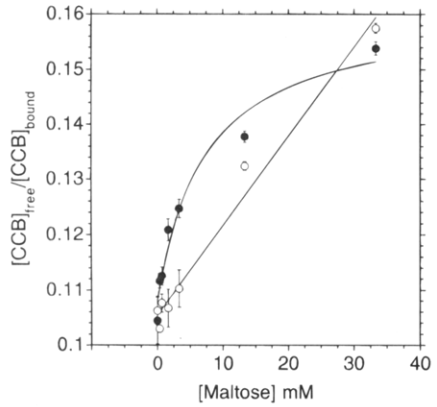

FIGURE 5: Effect of 2 mM DTT treatment of red cells on maltose inhibition of cytochalasin B binding. Ordinate: $[\text{cytochalasin B}]_{free}/[\text{cytochalasin B}]_{bound}$. Abscissa: $[\text{maltose}]_o$ in millimolar. The curves drawn through the data points assume that control cells (filled symbols) display negative, heterotropic cooperativity between maltose and cytochalasin B binding sites (Helgerson & Carruthers, 1987) with a K_o for maltose binding of 3.6 ± 0.1 mM, a $K_{d(app)}$ for CCB binding of 90 ± 12 nM, and a cooperativity factor, α, of 2.1 ± 0.1. The line drawn through the DTT data (open symbols) assumes simple competitive inhibition between cytochalasin B and maltose binding sites with a K_o for maltose binding of 32.5 ± 5.4 mM and a $K_{d(app)}$ for CCB binding of 90 ± 6 nM. These data summarize seven separate experiments. Each data point represents mean ± SEM of seven separate measurements made in quadruplicate.

negative-allosteric inhibition to simple, linear competitive inhibition (Figure 5).

Although exposure to reductant rapidly and reversibly modifies glucose transporter function and ligand binding in intact red cells, it is difficult to known whether transporter structure is affected at the same time. To address this question, we fixed red cells that were preincubated at 37 °C in the presence or absence of 2 mM DTT. These cells were attached to polylysine-coated coverslips prior to exposure to medium and fixative. The fixed cells were permeabilized, washed free of reductant, and stained separately either for tetrameric GLUT1-specific epitopes (using δ-Ab) or for total GLUT1 (using C-Ab), and the resulting staining intensities were visualized and quantitated using digital imaging fluorescence microscopy (Figure 6). While C-Ab binding is unaffected by cellular exposure to reductant, δ-Ab binding is reduced (3.5 ± 0.2)-fold by prior cell exposure to 2 mM DTT. Similar experiments were carried out using CHO cells, but here cells were dual-stained for δ- and C-Ab reactive epitopes. CHO cells (growing on coverslips) were exposed to saline or to saline plus 2 mM DTT, fixed, washed free of DTT, and permeabilized prior to staining. The CHO cell δ- and C-Ab binding images shown in Figure 6 (e.g., panels e and f) were obtained simultaneously from the same field. DTT inhibits δ-Ab binding to CHO cells by 76%. As with red cells, C-Ab binding is unaffected by prior DTT exposure.

In parallel experiments, 2 mM DTT inhibits 2-deoxy-D-glucose net uptake at 22 °C by 2-fold in parental CHO-K1 cells and in CHO cells overexpressing GLUT1 (CWT cells; Table 3). 2-Deoxy-D-glucose phosphorylation is rate-limiting for net uptake in these experiments [$t_{1/2}$ for CHO cell uptake of the nonmetabolized sugar 3-*O*-methylglucose (100 μM) at 4 °C is 40 s]. While we cannot rule out the possibility that DTT affects the 2-deoxy-D-glucose phosphorylation step and not transport, this appears unlikely since the redox state of cytosol in viable cells is reducing in the absence of exogenous reductant (Gilbert, 1982).

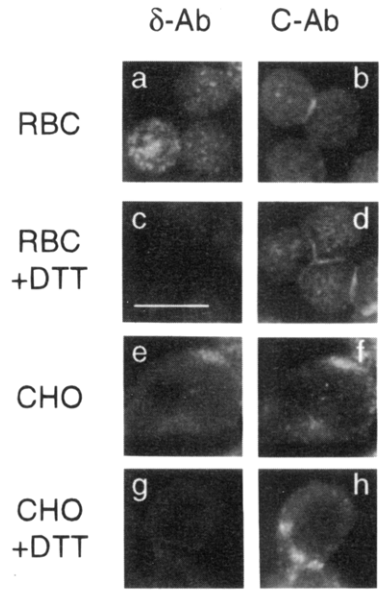

FIGURE 6: Images show red cells (RBC, panels a−d) and CHO cells (panels e−h) fixed in the presence (c, d, g, h) or absence (a, b, e, f) of 2 mM DTT. Cells were then washed and stained for δ-Ab (a, c, e, g) and/or C-Ab (b, d, f, h) reactive epitopes. Red cells were not stained simultaneously for δ-Ab and C-Ab binding sites. Thus, cells in panel a are not identical to those in panel b but are from the same population of cells and were processed in parallel to cells in panel a. CHO cells were dual-stained for ∂-Ab (panels e, g) and C-Ab (panels f, h) reactive epitopes. Thus, images shown in panels e and f show δ-Ab and C-Ab binding associated fluorescence, respectively, from the same cells. Exposure to DTT prior to fixation inhibits δ-Ab binding by as much as 4-fold. As with Figure 2 and for display purposes only, the full range of fluorescence intensities associated with all images acquired using a given primary antiserum and cell type is compressed to a scale of 0−255 (8-bit resolution). The actual (measured) range of fluorescence intensities in these experiments is (panels a and c) 0−3164 (arbitrary units), (panels b and d) 0−4281, (panels e and g) 0−3729, and (panels f and h) 0−1462. These results are typical of three separate experiments.

DISCUSSION

The facilitated diffusion of sugars across cell membranes is usually attributed (Bell et al., 1993; Mueckler, 1993) to a protein-mediated, uniport (transport) mechanism called the simple carrier. According to this model, transport is a sequential (iso-uni ping-pong) process in which the transporter (E) cycles between sugar import (E2) and sugar export (E1) states (Lieb & Stein, 1974; Widdas, 1952). While this model quantitatively predicts the steady-state sugar transport of some cells, it was recognized by Miller in 1968 (Miller, 1968) that key aspects of erythrocyte sugar transport are incompatible with this mechanism. This promoted systematic analyses of red cell sugar transport in which a number of groups ultimately rejected the simple carrier mechanism for erythrocyte hexose transport (Baker & Naftalin, 1979; Eilam & Stein, 1972; Ginsburg & Stein, 1975; Hankin et al., 1972; Holman, 1980; Holman et al., 1981; Lieb, 1982; Lieb & Stein, 1974; Naftalin & Holman, 1977; Stein, 1986). This conclusion stimulated unfavorable criticism and led others to reexamine earlier studies and subsequently to conclude that the simple carrier mechanism is an adequate description for erythrocyte sugar transport (Lowe & Walmsley, 1986; Wheeler, 1986; Wheeler & Whelan, 1988).

These later studies examine steady-state, unrestrained sugar transport in red cells. It had been recognized for some time, however (Baker & Widdas, 1973; Baker & Carruthers, 1981;

Krupka & Devés, 1981), and later proven theoretically (Carruthers, 1991), that such analyses often lack the sensitivity to distinguish various transport mechanisms. For example, theory shows that when cellular steady-state sugar transport is consistent with the simple carrier mechanism, it is always compatible by default with a diametric transport mechanism called the simultaneous or two-site carrier (Carruthers, 1991). This carrier, unlike the simple carrier, can bind sugars at import and export sites simultaneously (Baker & Widdas, 1973). The only acceptable conclusion these later studies allow is that steady-state red cell sugar transport could be mediated by both simple and simultaneous carrier mechanisms.

More sensitive tests of carrier mechanisms examine sugar heteroexchange (Miller, 1968) or inhibitions of sugar transport produced by the simultaneous presence of reversible competitive inhibitors of sugar import and export (Krupka & Devés, 1981). The results of these analyses are either consistent with simple and simultaneous carrier models (Krupka & Devés, 1981) or support rejection of the simple carrier (Carruthers & Helgerson, 1991; Helgerson & Carruthers, 1989; Miller, 1968; Naftalin & Rist, 1994; Naftalin et al., 1985). A single analysis of pre-steady-state sugar transport by red cells has been reported (Lowe & Walmsley, 1987), and the results are incompatible with the simple carrier mechanism (Naftalin, 1988).

A plausible, physical explanation for the complex kinetic behavior of the transporter was suggested when the erythrocyte sugar transporter was found to be an allosteric, oligomeric complex of four GLUT1 proteins (Hebert & Carruthers, 1991, 1992). This complex is stabilized by noncovalent subunit interactions but dissociates into GLUT1 dimers upon exposure to reductant. GLUT1 dimers function as prototypic simple carriers in which each subunit contributes a single transport unit (Appleman & Lienhard, 1989; Hebert & Carruthers, 1992). The parental transporter consists of four such subunits whose behavior in the mature complex is hypothesized (Hebert & Carruthers, 1992) to be constrained by subunit interactions. Cooperative interactions are suggested to produce a *pseudo-D2* symmetry in import and export site orientation within the transporter complex. When one subunit presents an import site, the adjacent subunit must expose an export site and *vice versa*. In this way, the parental transporter always exposes two sugar import and two sugar export sites although at any instant the individual subunits contributing specific sites vary.

According to this hypothesis, subunits of the parental transporter complex can now bypass rate-limiting steps in the ping-pong transport cycle and are thus more efficient catalytically than their dimeric counterparts. This hypothesis is supported indirectly by analyses of the catalytic turnover of dimeric GLUT1 (Appleman & Lienhard, 1989) and parental transporter (Lowe & Walmsley, 1986) at 10 °C which show that dimeric GLUT1 is some 10-fold less active than the parental transporter (Hebert & Carruthers, 1992).

This hypothesis has been questioned by Burant and Bell (1992), who conclude that sugar transporters exist functionally as monomeric species in the plasma membrane. However, the conclusion of Burant and Bell was based upon two indirect observations and five untested central assumptions. The observations are as follows: (1) coexpression of GLUT1 and GLUT3 in *Xenopus* oocytes results in expression of two kinetically distinct components of sugar uptake; (2) coexpression of wild-type GLUT3 and a mutagenized (dysfunctional) GLUT3 does not inhibit wild-type GLUT3 function. The untested assumptions were the following: (1) posttranslational processing of glucose transport proteins is identical in *Amphibia* and *Mammalia*; (2) glucose transporter isoforms and mutants share identical spatial and temporal processing kinetics (i.e., the proteins can oligomerize prior to insertion at the plasma membrane); (3) sugar transporters constantly dissociate and reoligomerize at the plasma membrane; (4) subunits of oligomeric transporters are *functionally* coupled at all times; (5) transporter isoforms can form heterocomplexes.

Recent findings invalidate the first two assumptions. In contrast to CHO cells (Pessino et al., 1991), GLUT1 and GLUT1/GLUT4 chimeras do not physically associate in *Xenopus* oocytes where the kinetics of isoform and mutant transporter processing can differ dramatically (Hresko et al., 1994). Our earlier studies (Hebert & Carruthers, 1991, 1992) demonstrate that the third assumption is invalid in erythrocytes and CHO cells. A number of studies argue against obligate functional coupling between transporter subunits and thus refute the fourth assumption. For example, dimeric GLUT1 consists of structurally coupled but functionally independent GLUT1 proteins (Hebert & Carruthers, 1991, 1992). Expression of dysfunctional GLUT1 mutants by CHO cells can be without effect on parental GLUT1 function (Tamori et al., 1994) or can inhibit parental GLUT1 functions (Mori et al., 1994)—the effect is mutant-specific. The fifth assumption is refuted by earlier studies showing that GLUT1 and GLUT4 do not form heterocomplexes (Pessino et al., 1991).

A substantial body of direct, biophysical evidence supports the hypothesis that GLUT1 exists as an oligomeric complex (Hebert & Carruthers, 1991, 1992; Jarvis et al., 1986; Jung et al., 1980; Pessino et al., 1991; Sogin & Hinkle, 1978; Zoccoli et al., 1978). The present study was formulated to answer two questions: (1) Why is the quaternary structure of the glucose transporter sensitive to reductant if it is stabilized primarily through noncovalent subunit interactions? (2) Do cooperative subunit interactions truly increase the catalytic efficiency of tetrameric GLUT1? Our findings support the hypothesis that each subunit (GLUT1 protein) of the parental glucose transporter contains a single intramolecular disulfide bridge between cysteine residues 347 and 421. This disulfide seems to be necessary for GLUT1 tetramerization. Our findings suggest that GLUT1 N-terminal residues 1−199 provide contact surfaces for subunit dimerization but are insufficient for subunit tetramerization. Our studies also show that *in situ* disulfide disruption by chemical or recombinant means results in the loss of cooperative subunit interactions and a 3−15-fold reduction in the intrinsic efficiency of the transporter. We will, however, discuss two key experiments that show that GLUT1 catalytic efficiency does not derive directly from cooperative interactions between substrate binding sites on adjacent subunits.

Quantitation of GLUT1 disulfide content first requires sulfitolysis of disulfides followed by quantitation of exposed thiols by the NTSB assay (Rao & Scarborough, 1990). Disulfide cleavage by sulfitolysis produces one S-sulfonated cysteine and reveals a free thiol group on the remaining cysteine. The assay for an internal disulfide thus yields 1 mol of NTB/2 mol of internal cysteine while that for a mixed disulfide yields 1 mol of NTB/mol of internal cysteine. Our assay detects 4.8 ± 0.3 mol of NTB, which, since parental

GLUT1 exposes two sulfhydryl groups without prior reduction, indicates that sulfitolysis reveals an additional 3 mol of reactive sites. This result strongly suggests that GLUT1 contains one internal disulfide and either two mixed disulfides or two free sulfhydryl groups that are revealed only when the disulfide bridge is broken. It is unlikely that the "missing" thiol is inaccessible due to covalent modification by other species since DTT reveals this group. It is unlikely that sulfitolysis is incomplete since excess (10 000-fold) sodium sulfite was used and GLUT1 (which was unfolded in SDS) is quantitatively alkylated under similar conditions.

N-Terminal sequence and immunoblot analyses of [^{14}C-] iodoacetic acid labeled GLUT1 peptides indicate that a C-terminal peptide containing GLUT1 residues 233−492 contains three of the four inaccessible sulfhydryl groups of each parental GLUT1 subunit while a peptide containing GLUT1 residues 147−260/299 contains both reactive thiols. The conditions used here for GLUT1 alkylation do not favor alkylation of other functional groups (Gurd, 1972), and quantitation of presumed GLUT1 *S*-(carboxymethyl)cysteine content is in agreement with GLUT1 sulfhydryl content as measured using Ellman's reagent. It is unlikely, therefore, that these quantitative estimates are seriously flawed. The mobility of the GLUT1 C-terminal fragment is unaffected by omission of reductant during electrophoresis. If the peptide were to remain disulfide-linked to the smallest possible GLUT1 tryptic fragments containing either cysteine 133 (residues 184−212) or cysteines 201 and 207 (residues 127−153), its molecular mass would increase by 3308 or by 2925 daltons, respectively. No mobility shift is detected even though molecular mass markers of the same range of molecular mass but differing by only 5000 daltons are clearly separated.

May has shown that GLUT1 cysteine 429 can be alkylated by cell-impermeant maleimides (May, 1988; May et al., 1990). However, alkylation is not quantitative and ranges between 2 and 14 mol % incorporation (May et al., 1990). This is consistent with our estimates of the molar incorporation of iodoacetic acid into the carboxyl-terminal GLUT1 peptide (20 mol %). In independent studies using a *Xenopus* oocyte expression system, Wellner and colleagues (Wellner et al., 1992, 1994) have demonstrated that GLUT1 cysteine 429 is required for exofacial pCMBS inhibition of sugar transport but suggest that mutagenesis of individual cysteine residues is without effect on sugar uptake by GLUT1 expressed in *Xenopus* oocytes. These studies do not permit direct comparison of the catalytic activities of the various GLUT1 cysteine mutants in *Xenopus* oocytes since the cell-surface GLUT1 content was not quantitated and transport was measured at only one or two sugar concentrations. However, if GLUT1 cysteine mutants are not inhibited, this suggests either (1) that the cysteine hypothesis is incorrect or (2) that GLUT1 does not fold normally in oocytes. Recent experiments from this laboratory show[2] that GLUT1 expressed in oocytes is capable of transporting sugars but neither binds ∂-Ab nor is inhibited by dithiothreitol. This strongly suggests that the structural and functional phenotype of oocyte-expressed GLUT1 differs fundamentally from that of human erythrocyte and CHO cell GLUT1. Oocyte-expressed GLUT1 may resemble dimeric GLUT1—an *in vitro*, low-affinity form of the erythrocyte sugar transporter (Hebert & Carruthers, 1992). This would explain the troubling observation that oocyte-expressed GLUT1 binds sugars with 5−10-fold lower affinity than does erythroid GLUT1 (Burant & Bell, 1992).

In the studies reported here, immunoblot and immunohistochemistry analyses of parental and transfected CHO cell GLUT1 content show that wild-type GLUT1 and GLUT1 cysteine mutants are expressed at levels 2−5-fold greater than is endogenous GLUT1. We selected the highest overexpressers for analysis of GLUT1 oligomeric structure. The least ambiguous method for determining the oligomeric state of CHO cell GLUT1 would be to perform hydrodynamic size analyses on purified, solubilized GLUT1. This method requires additional quantitation of micellular lipid and detergent content and suffers from the potential for purification-associated perturbations in transporter quaternary structure [see Hebert and Carruthers (1992)]. An alternative approach is to perform hydrodynamic size analyses of GLUT1 solubilized directly from CHO cell membranes. This approach, although useful, is not definitive since the protein, detergent, and lipid contents of the solubilized GLUT1-containing micelles are uncertain. The strategy we adopted was to quantitate binding of an antitetrameric GLUT1 antiserum (δ-Ab) to CHO cell GLUT1 and to contrast this binding with that of an antiserum (C-Ab) that shows no detectable sensitivity to GLUT1 quaternary structure (Hebert & Carruthers, 1992).

We have previously demonstrated that δ-Ab does not cross-react with dimeric GLUT1 but binds with high affinity to tetrameric GLUT1 (Hebert & Carruthers, 1992) and to SDS-denatured, reduced GLUT1 (Harrison et al., 1990a). We have demonstrated that δ-Ab binding to CHO cells is directly proportional to CHO-cell GLUT1 expression over a 20-fold range (Harrison et al., 1990a) and that δ-Ab binds at an exofacial site(s) on the transporter (Harrison et al., 1990a). We have further shown that reversible dissociation of tetrameric GLUT1 into dimeric GLUT1 is associated with the reversible loss of δ-Ab binding to GLUT1 (Hebert & Carruthers, 1992). We have also shown that affinity purification of δ-Ab using reduced, SDS-unfolded GLUT1 results in quantitative recovery of binding activity to intact cells (Coderre et al., 1995). Together these data suggest that GLUT1 contains specific epitopes that are exposed in tetrameric GLUT1 but not in the GLUT1 dimer. Thus, the ability of δ-Ab to bind to GLUT1 reflects the accessibility of these epitopes. It is possible that δ-Ab-reactive epitopes could be sequestered or exposed in the absence of any change in transporter oligomeric structure. This has not been observed experimentally (Coderre et al., 1995; Hebert & Carruthers, 1992).

Our results show that serine substitution at cysteines 347 and 421 significantly reduces δ-Ab binding to GLUT1. The magnitude of this effect suggests that the remaining δ-Ab binding is accounted for by binding to parental GLUT1. While these results do not discount the possibility that serine substitution at cysteines 347 and 421 induces subtle conformational changes that mask the δ-Ab epitopes, they are consistent with the view that these cysteine residues are important for GLUT1 oligomeric structure. When reviewed in the context of the peptide mapping/alkylation studies, these finding strongly suggest that the internal, GLUT1 disulfide bridge, if extant, is formed between residues 347 and 421.

Hydrodynamic analyses using GLUT1/GLUT4 chimeras indicate that GLUT1 residues 463−492 make a negligible

[2] R. J. Zottola, E. K. Cloherty, and A. Carruthers, unpublished observations.

(isoform-specific) contribution to GLUT1 oligomeric structure. This is consistent with the observation that anti-GLUT1 carboxyl-terminal peptide antiserum (C-Ab) binding to GLUT1 is insensitive to GLUT1 oligomeric structure. A portion (25%) of the expressed GLUT1n-4 chimera (GLUT1 residues 1−199 plus GLUT4 residues 216−509) does resolve as a tetramer. Specific immunoprecipitation of GLUT1n-4 from CHO cells using anti-GLUT4 carboxyl-terminal peptide antiserum quantitatively precipitates parental GLUT1 (Pessino et al., 1991). Almost all parental GLUT1 from GLUT1n-4 chimera-expressing cells coresolves with authentic tetrameric GLUT1. However, most of the chimera coresolves with authentic dimeric GLUT1. While our studies cannot rule out the possibility that GLUT1n-4-containing micelles contain molecular species other than lipid, detergent, GLUT1n-4, and GLUT1, these data are consistent with the hypothesis that GLUT1n-4/wild-type GLUT1 complexes are heterotetramers while the remaining GLUT1n-4 forms only homodimeric structures. If correct, this would mean that wild-type GLUT1 is dominant-positive over GLUT1n-4 with regard to transporter oligomeric structure.

These data further suggest that the GLUT1 N-terminal half provides dimerization motifs/contact surfaces while the carboxyl-terminal half contains the tetramerization motif (Cys347 and Cys421) and contact surfaces. These contact surfaces for tetramerization presumably also include domains that are well conserved in GLUT1 and GLUT4 carboxyl-terminal halves. GLUT1 residues 200−463 and GLUT4 residues 216−479 share 78% sequence homology.

We have previously hypothesized (Hebert & Carruthers, 1992) that tetrameric GLUT1 is a more efficient transporter than its reduced, dimeric counterpart. This hypothesis is based on kinetic analyses of red cell resident (tetrameric) GLUT1 and reduced, purified GLUT1 (Appleman & Lienhard, 1989; Lowe & Walmsley, 1986) that show that the catalytic turnover of purified dimeric GLUT1 at 10 °C is significantly lower than that of red cell resident GLUT1 at the same temperature. Specifically, dimer-mediated net uptake and net exit are 2-fold and 8-fold slower, respectively, than those mediated by native GLUT1. While omission of a number of extrinsic environmental factors can be offered for the catalytic deficit of reduced purified GLUT1, a kinetic rationale for this behavior is provided by the observation that exchange transport (sugar uptake coupled to sugar exit) by dimeric and native GLUT1 is indistinguishable. This indicates that sugar-promoted translocation steps are largely insensitive to transporter oligomeric structure. It is the sugar-independent, transporter conformational changes (relaxation steps) inferred to be sensitive to transporter oligomeric structure. The slowest steps catalyzed by dimeric GLUT1 are relaxation steps (E1 ↔ E2) which, at 10 °C, occur almost 100-fold more slowly than do the sugar translocation steps (E·S1 ↔ E·S2) (Appleman & Lienhard, 1989). If the transporter could bypass relaxation steps, transport would be stimulated dramatically. In principle, this is what tetrameric GLUT1 (a simultaneous carrier) should achieve since the simultaneous carrier couples sugar import and regeneration of import sites into a single step.

The current study tested this hypothesis by exposing erythrocyte-resident GLUT1 to reductant. This reduces the intramolecular disulfide bridge of each subunit, causing the transporter to dissociate into dimers (Coderre et al., 1995). In this way, the catalytic and ligand binding properties of the dimer and tetramer can be contrasted directly. Tetrameric GLUT1 dissociation into dimers should be accompanied by a loss of δ-Ab binding to red cells. C-Ab binding to permeabilized cells, however, should be unchanged since this antiserum recognizes an epitope whose availability is insensitive to GLUT1 oligomeric structure. Our results show that red cell fixation in the presence of reductant significantly reduces the availability of the δ-Ab-specific epitope(s) while C-Ab binding is unchanged. Assuming the loss of δ-Ab binding reflects GLUT1 dissociation into dimers, the cooperativity hypothesis predicts that the ligand binding and sugar transport properties of the cells will be modified dramatically.

Transporter conversion from a simultaneous carrier (tetramer) to a simple carrier (dimer) will impact cytochalasin B binding to GLUT1 in two ways. GLUT1 cytochalasin B binding capacity will be doubled and inhibition of cytochalasin B binding to GLUT1 by extracellular maltose will be transformed from complex allosteric inhibition to simple competitive inhibition. Increased cytochalasin B binding is expected because only half of the subunits of tetrameric GLUT1 can present an export (cytochalasin B binding) site at any instant. When tetrameric GLUT1 dissociates into dimers, subunits are released from this constraint and now isomerize independently of their neighbor. Thus, each subunit now presents an export site and therefore binds cytochalasin B independently of its neighbor. This prediction was satisfied experimentally.

Inhibitions of ligand binding to tetrameric GLUT1 may be competitive or allosteric depending on the sites of action. For example, inhibition of extracellular maltose binding by extracellular D-glucose would be competitive because both ligands compete for the import site (an E2 subunit conformation). Similarly, inhibition of cytochalasin B binding by intracellular D-glucose would be competitive since cytochalasin B binds at or close to the sugar export site (an E1 subunit conformation). Extracellular maltose inhibition of cytochalasin B binding to tetrameric GLUT1, however, requires negative cooperative interactions between subunits. Thus, maltose binding to an E2 subunit will affect cytochalasin B binding to an E1 subunit only if the occupancy state of the E2 subunit is communicated to adjacent E1 subunits and vice versa. In dimeric GLUT1, each subunit functions independently of its neighbor as an E1 or E2 conformation. Cytochalasin B binding to E1 will competitively inhibit maltose binding to E2 and vice versa. Our experiments demonstrate that dithiothreitol converts maltose inhibition of cytochalasin B binding from negative allosteric inhibition to simple competitive inhibition.

3-*O*-Methylglucose uptake is noncompetitively inhibited following red cell exposure to reductant. The extent of import inhibition ranges from 3- to 16-fold and is rapidly reversed upon removal of extracellular reductant. Transport inhibition increases in the order dithiothreitol < β-mercaptoethanol < reduced glutathione. Transport inhibition is not observed in resealed erythrocyte ghosts that contain 2 mM DTT but are washed free of extracellular reductant. These findings indicate that the site of action is most likely extracellular and that inhibition is unrelated to the closed-ring structure of oxidized dithiothreitol.

An unexpected result is the failure of reductant to inhibit erythrocyte sugar efflux. This suggests a number of possibilities: (1) the cooperativity hypothesis is incorrect; (2) purified reduced GLUT1 is unable to mimic faithfully the catalytic properties of erythrocyte-resident, reductant-exposed GLUT1; (3) the observed kinetics of erythrocyte sugar exit

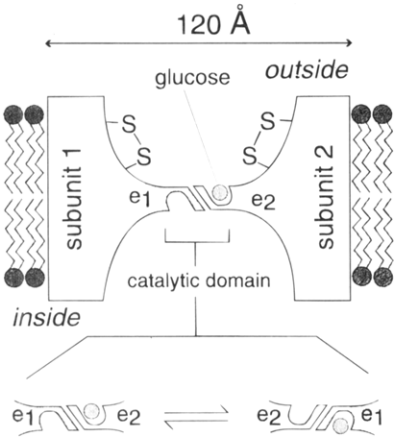

FIGURE 7: Hypothetical glucose transporter is shown looking into the plane of the bilayer. The section is across two of the four subunits that form the transporter. The complex forms a water-filled cavity that almost extends across the entire bilayer. Dimensions are based in part upon measured hydrodynamic radii and detergent/lipid/protein ratios of GLUT1 micelles (Hebert & Carruthers, 1992). The catalytic domain is at the center of the water-filled cavity. Each subunit contributes one transport site to the complex (these domains and their conformational changes are shown in expanded view at the bottom of the figure). Subunit 1 is shown in an e1 state (exposing an intracellular sugar binding site and shaded for clarity) while subunit 2 is in an e2 state (binding extracellular sugar). When subunit 2 translocates its bound sugar across the membrane (an e2 ↔ e1 conformational change), subunit 1 must undergo the antiparallel (e1 ↔ e2) conformational change and *vice versa*. In this way, the transporter complex always exposes two sugar influx sites and two sugar efflux sites. The structure of each subunit is stabilized by an extracellular, internal disulfide between cysteine residues 347 and 421. Reduction of this bridge results in tetramer dissociation into dimers. Reduced subunits adopt an altered conformation that causes the loss of functional coupling between adjacent catalytic sites. Each site can now isomerize between e1 and e2 states without affecting (and independently of) the state of its neighbor.

do not reflect the intrinsic catalytic properties of the transporter. Ample evidence supports the latter two possibilities. The absence of nucleotides (AMP, ADP, ATP) impacts the behavior of purified GLUT1 since the transporter is also a nucleotide binding protein (Carruthers & Helgerson, 1989; Helgerson et al., 1989) whose catalytic turnover and ligand binding properties are radically altered in the presence of nucleotide (Carruthers, 1986a,b; Carruthers & Helgerson, 1989; Carruthers & Melchior, 1983; Helgerson et al., 1989; Jacquez, 1983). In addition, kinetic analysis suggests that intracellular sugar is distributed between free and bound compartments (Helgerson & Carruthers, 1989; Naftalin et al., 1985; Nishimura et al., 1993). The observable kinetics of transport (which assume that all intracellular sugar is free) are, therefore, unlikely to accurately reflect the intrinsic behavior of the transporter.

One additional study, however, supports rejection of the cooperativity hypothesis. Coderre et al. (1995) have demonstrated that exofacial proteolysis of GLUT1 abolishes cooperativity in ligand binding to GLUT1 but fails to impact GLUT1 oligomeric structure or sugar transport function. This suggests, therefore, that rapid substrate translocation by parental (tetrameric) GLUT1 results from subunit interactions distinct from those that promote cooperative ligand binding.

We propose a model (Figure 7) in which the native transporter is a GLUT1 tetramer. This structure is stabilized by a single, extracellular disulfide bridge within each subunit. Contacts between subunits are of two types. Dimerization surfaces are provided by the N-terminal 199 residues of GLUT1. Tetramerization and cooperativity contacts are provided by GLUT1 carboxyl-terminal residues 200−463. The disulfide bridge between cysteine residues 347 and 421 spans the proposed ligand binding/catalytic domain of GLUT1 (Clark & Holman, 1990; Deziel et al., 1984; Holman et al., 1988; Holman & Rees, 1987; Karim et al., 1987; Oka et al., 1991) and is thus well positioned to impact the ligand binding and catalytic properties of each subunit. Like the potassium channel of the endoplasmic reticulum (Miller, 1982) and the erythrocyte water channel (Smith & Agre, 1991), we suggest that the catalytic domain of GLUT1 does not span the entire membrane but, rather, is formed from a limited structure that bridges a larger, water-filled cavity. This is consistent with the very high (>80%) solvent accessibility of the GLUT1 polypeptide backbone (Alvarez et al., 1987; Jung et al., 1986) and the amphiphatic nature of a number of proposed membrane-spanning domains (Mueckler et al., 1985). This hypothesis is also consistent with the observation that GLUT1-mediated sugar transport is a diffusion-limited process (Cloherty et al., 1995) and allows for disulfide bridge formation within protein domains hypothesized previously to be buried within the lipid bilayer and thus inaccessible to extracellular solvent.

ACKNOWLEDGMENT

We thank Dr. Frederick Fay and the Biomedical Imaging Group of Dr. Frederick Fay's laboratory for helpful discussions. The comments of a reviewer were most helpful in the preparation of the manuscript.

REFERENCES

Agard, D. A., Hiraoka, Y., Shaw, P., & Sedat, J. W. (1989) *Methods Cell Biol. 30*, 353−377.
Alvarez, J., Lee, D. C., Baldwin, S. A., & Chapman, D. (1987) *J. Biol. Chem. 262*, 3502−3509.
Anderson, C. M., Zucker, F. H., & Steitz, T. A. (1979) *Science 204*, 375−380.
Appleman, J. R., & Lienhard, G. E. (1989) *Biochemistry 28*, 8221−8227.
Arce, M. A., Thompson, E. S., Wagner, S., Coyne, K. E., Ferdman, B. A., & Lublin, D. M. (1993) *Blood 82*, 651−655.
Baker, G. F., & Widdas, W. F. (1973) *J. Physiol. (London) 231*, 143−165.
Baker, G. F., & Naftalin, R. J. (1979) *Biochim. Biophys. Acta 550*, 474−484.
Baker, P. F., & Carruthers, A. (1981) *J. Physiol. (London) 316*, 503−525.
Baldwin, S. A., Baldwin, J. M., Gorga, F. R., & Lienhard, G. E. (1979) *Biochim. Biophys. Acta 552*, 183−188.
Baldwin, S. A., Baldwin, J. M., & Lienhard, G. E. (1982) *Biochemistry 21*, 3836−3842.
Barnett, J. E., Holman, G. D., & Munday, K. A. (1973) *Biochem. J. 131*, 211−221.
Bell, G. I., Burant, C. F., Takeda, J., & Gould, G. W. (1993) *J. Biol. Chem. 268*, 19161−19164.
Brown, R. E., Jarvis, K. L., & Hyland, K. J. (1989) *Anal. Biochem. 180*, 136−139.
Burant, C. F., & Bell, G. I. (1992) *Biochemistry 31*, 10414−10420.
Cairns, M. T., Elliot, D. A., Scudder, P. R., & Baldwin, S. A. (1984) *Biochem. J. 221*, 179−188.
Carruthers, A. (1986a) Biochemistry *25*, 3592−3602.
Carruthers, A. (1986b) *J. Biol. Chem. 261*, 11028−11037.
Carruthers, A. (1991) *Biochemistry 30*, 3898−3906.
Carruthers, A., & Melchior, D. L. (1983) *Biochim. Biophys. Acta 728*, 254−266.
Carruthers, A., & Halgerson, A. L. (1989) *Biochemistry 28*, 8337−8346.

Carruthers, A., & Helgerson, A. L. (1991) *Biochemistry 30*, 3907−3915.
Chin, J. J., Jhun, B. H., & Jung, C. Y. (1992) *Biochemistry 31*, 1945−1951.
Clark, A. E., & Holman, G. D. (1990) *Biochem. J. 269*, 615−622.
Cloherty, E. K., Sultzman, L. A., Zottola, R. J., & Carruthers, A. (1995) *Biochemistry* (submitted for publication).
Coderre, P. E., Cloherty, E. K., Zottola, R. J., & Carruthers, A. (1995) *Biochemistry* (in press).
Deziel, M., Pegg, W., Mack, E., Rothstein, A., & Klip, A. (1984) *Biochim. Biophys. Acta 772*, 403−406.
Eilam, Y., & Stein, W. D. (1972) *Biochim. Biophys. Acta 266*, 161−173.
Freshney, R. I. (1994) in *Culture of Animal Cells*, 3rd ed., pp 169−171, Wiley-Liss, New York.
Gilbert, H. F. (1982) *J. Biol. Chem. 257*, 12086−12091.
Ginsburg, H., & Stein, D. (1975) *Biochim. Biophys. Acta*, 353−368.
Glynn, I. M., & Richards, D. E. (1982) *J. Physiol. (London) 330*, 17−43.
Glynn, I. M., Hara, Y., & Richards, D. E. (1984) *J. Physiol. (London) 351*, 531−547.
Gurd, F. R. N. (1972) *Methods Enzymol. 25*, 424−438.
Ham, R. G. (1965) *Proc. Natl. Acad. Sci. U.S.A. 53*, 288−294.
Hankin, B. L., Lieb, W. R., & Stein, W. D. (1972) *Biochim. Biophys. Acta 288*, 114−126.
Harrison, S. A., Buxton, J. M., Helgerson, A. L., MacDonald, R. G., Chlapowski, F. J., Carruthers, A., & Czech, M. P. (1990a) *J. Biol. Chem. 265*, 5793−5801.
Harrison, S. A., Buxton, J. M., Clancy, B. M., & Czech, M. P. (1990b) *J. Biol. Chem. 265*, 20106−20116.
Hebert, D. N., & Carruthers, A. (1991) *Biochemistry 30*, 4654−4658.
Hebert, D. N., & Carruthers, A. (1992) *J. Biol. Chem. 267*, 23829−23838.
Helgerson, A. L., & Carruthers, A. (1987) *J. Biol. Chem. 262*, 5464−5475.
Helgerson, A. L., & Carruthers, A. (1989) *Biochemistry 28*, 4580−4594.
Helgerson, A. L., Hebert, D. N., Naderi, S., & Carruthers, A. (1989) *Biochemistry 28*, 6410−6417.
Holman, G. D. (1980) *Biochim. Biophys. Acta 599*, 202−213.
Holman, G. D., & Rees, W. D. (1987) *Biochim. Biophys. Acta 897*, 395−405.
Holman, G. D., Busza, A. L., Pierce, E. J., & Rees, W. D. (1981) *Biochim. Biophys. Acta 649*, 503−514.
Holman, G. D., Karim, A. R., & Karim, B. (1988) *Biochim. Biophys. Acta 946*, 75−84.
Hresko, R. C., Murata, H., Marshall, B. A., & Mueckler, M. (1994) *J. Biol. Chem. 269*, 32110−32119.
Jacquez, J. A. (1983) *Biochim. Biophys. Acta 727*, 367−378.
Janoshazi, A., & Solomon, A. K. (1993) *J. Membr. Biol. 132*, 167−178.
Janoshazi, A., Kifor, G., & Solomon, A. K. (1991) *J. Membr. Biol. 123*, 191−207.
Marvis, S. M., Ellory, J. C., & Young, J. D. (1986) *Biochim. Biophys. Acta 855*, 312−315.
Jung, C. Y., & Rampal, A. L. (1977) *J. Biol. Chem. 252*, 5456−5463.
Jung, C. Y., Hsu, T. L., Cha, J. S., & Haas, M. N. (1980) *J. Biol. Chem. 225*, 361−364.
Jung, E. K. Y., Chin, J. J., & Jung, C. Y. (1986) *J. Biol. Chem. 261*, 9155−9160.
Karim, A. R., Rees, W. D., & Holman, G. D. (1987) *Biochim. Biophys. Acta 902*, 402−405.
Kasahara, M., & Hinkle, P. C. (1977) *J. Biol. Chem. 253*, 7384−7390.
Kondo, T., Miyamoto, K., Gasa, S., Taniguchi, N., & Kawakami, Y. (1989) *Biochem. Biophys. Res. Commun. 162*, 1−8.
Krupka, R. M., & Devés, R. (1981) *J. Biol. Chem. 256*, 5410−5416.
Leventis, R., & Silvius, J. R. (1990) *Biochim. Biophys. Acta 1023*, 124−132.
Lieb, W. R. (1982) in *Red Cell Membranes. A Methodological Approach* (Young, J. C. E., Ed.) pp 135−164, Academic Press, New York.
Lieb, W. R., & Stein, W. D. (1974) *Biochim. Biophys. Acta 373*, 178−196.
Lowe, A. G., & Walmsley, A. R. (1986) *Biochim. Biophys. Acta 857*, 146−154.
Lowe, A. G., & Walmsley, A. R. (1987) *Biochim. Biophys. Acta 903*, 547−550.
May, J. M. (1988) *J. Biol. Chem. 263*, 13635−13640.
May, J. M., Buchs, A., & Carter, S. C. (1990) *Biochemistry 29*, 10393−10398.
Miller, C. (1982) in *Transport in Biomembranes* (Antolini, R., Gliozzi, A., & Gorio, A., Eds.) pp 99−108, Raven Press, New York.
Miller, D. M. (1968) *Biophys. J. 8*, 1329−1338.
Mori, H., Hashiramoto, M., Clark, A. E., Yang, J., Muraoka, A., Tamori, Y., Kasuga, M., & Holman, G. D. (1994) *J. Biol. Chem. 269*, 11578−11583.
Mueckler, M. (1993) *J. Diabetes Complications 7*, 130−141.
Mueckler, M., Caruso, C., Baldwin, S. A., Panico, M., Blench, I., Morris, H. R., Allard, W. J., Lienhard, G. E., & Lodish, H. F. (1985) *Science 229*, 941−945.
Naftalin, R. J. (1988) *Biochim. Biophys. Acta 946*, 431−438.
Naftalin, R. J., & Holman, G. D. (1977) in *Membrane Transport in Red Cells* (Ellory, J. C., & Lew, V. L., Eds.) pp 257−300, Academic Press, New York.
Naftalin, R. J., & Rist, R. J. (1994) *Biochim. Biophys. Acta 1191*, 65−78.
Naftalin, R. J., Smith, P. M., & Roselaar, S. E. (1985) *Biochim. Biophys. Acta 820*, 235−249.
Nakamaye, K., & Eckstein, F. (1986) *Nucleic Acids Res. 14*, 9679−9698.
Nishimura, H., Pallardo, F. V., Seidner, G. A., Vannucci, S., Simpson, I. A., & Birnbaum, M. J. (1993) *J. Biol. Chem. 268*, 8514−8520.
Oka, Y., Asano, T., & Katagiri, H. (1991) *J. Cell. Biochem. 15B*, CB 129.
Pessino, A., Hebert, D. N., Woon, C. W., Harrison, S. A., Clancy, B. M., Buxton, J. M., Carruthers, A., & Czech, M. P. (1991) *J. Biol. Chem. 266*, 20213−20217.
Rao, U. S., & Scarborough, G. A. (1990) *J. Biol. Chem. 265*, 7227−7235.
Smith, B. L., & Agre, P. (1991) *J. Biol. Chem. 266*, 6407−6415.
Sogin, D. C., & Hinkle, P. C. (1978) *J. Supramol. Struct. 8*, 447−453.
Srivastava, S. K., & Beutler, E. (1969) *J. Biol. Chem. 244*, 9−16.
Stein, W. D. (1986) in *Transport and Diffusion across Cell Membranes*, pp 231−305, Academic Press, New York.
Tamori, Y., Hashiramoto, M., Clark, A. E., Mori, H., Muraoka, A., Kadowaki, T., Holman, G. D., & Kasuga, M. (1994) *J. Biol. Chem. 269*, 2982−2986.
Wellner, M., Monden, I., & Keller, K. (1992) *FEBS Lett. 309*, 293−296.
Wellner, M., Monden, I., & Keller, K. (1994) *Biochem. J. 299*, 813−817.
Wheeler, T. J. (1986) *Biochim. Biophys. Acta 862*, 387−398.
Wheeler, T. J., & Whelan, J. D. (1988) *Biochemistry 27*, 1441−1446.
Widdas, W. F. (1952) *J. Physiol. (London) 118*, 23−39.
Zoccoli, M. A., Baldwin, S. A., & Lienhard, G. E. (1978) *J. Biol. Chem. 253*, 6923−6930.

BI950558X